

POWER LOAD FROM COLLISION DEBRIS ON THE LHC POINT 8 INSERTION MAGNETS IMPLIED BY THE LHCb LUMINOSITY INCREASE*

L. S. Esposito[†], F. Cerutti, A. Lechner, A. Mereghetti[‡], V. Vlachoudis, CERN, Geneva, Switzerland
A. Patapenka[§], JIPNR-Sosny NASB, Minsk, Russia

Abstract

LHCb is aiming to upgrade its goal peak luminosity up to a value of $2 \times 10^{33} \text{ cm}^{-2} \text{ s}^{-1}$ after LS2. We investigate the collision debris impact on the machine elements by extensive FLUKA simulations, showing that the present machine layout is substantially compatible with such a luminosity goal. In particular the installation of a TAS (Target Absorber of Secondaries, installed in front of the final focus Q1-Q3 quadrupole triplet in the LHC high luminosity insertions) turns out not to be necessary on the basis of the expected peak power deposition in the Q1 superconducting coils. A warm protection may be desirable to further reduce heat load and dose on the D2 recombination dipole, due to the absence of the TAN (Target Absorber of Neutrals, present in Point 1 and 5).

INTRODUCTION

The Large Hadron Collider (LHC) operated at CERN produced proton-proton interactions at a maximum center-of-mass energy $\sqrt{s} = 8 \text{ TeV}$ in 2012 operations. The maximum averaged luminosity delivered to the LHCb detector was about $4 \times 10^{32} \text{ cm}^{-2} \text{ s}^{-1}$. During the Long Shutdown 2 (LS2, CERN machine shutdown scheduled in 2018), the LHCb collaboration foresees to upgrade the detector in order to sustain a peak luminosity of $\mathcal{L}_{\text{max-LHCb}} = 2 \times 10^{33} \text{ cm}^{-2} \text{ s}^{-1}$ at $\sqrt{s} = 14 \text{ TeV}$ [1].

One concern related to operation at higher luminosity in LHCb is the risk of quench of the superconducting magnets in the Long Straight Section (LSS) induced by collision debris particles coming from the Interaction Point (IP). In the Insertion Region 8 (IR8), where the LHCb detector is located, no passive absorbers of secondaries have been installed because they were considered unnecessary below $\mathcal{L} = 10^{33} \text{ cm}^{-2} \text{ s}^{-1}$ [2]. Therefore, operation at higher luminosity requires further studies to estimate the heat deposition onto NbTi coils, namely of Inner Triplet (IT) quadrupoles and separation/recombination dipoles, in order to evaluate the risk of quench and to assess the need of the TAS (as shielding for the IT quadrupole magnets), and TAN (located in front of the D2 dipole magnet, to protect the Matching Section elements, mainly from neutral particles leaving the IP) absorbers.

* Research supported by the High Luminosity LHC project.

[†] Luigi.Salvatore.Esposito@cern.ch

[‡] also at UMAN, Manchester

[§] also at CERN, Geneva

FLUKA SIMULATION

IR8 has been modeled in FLUKA [3, 4] taking into account all the main elements along the beam line up to D2, including experimental spectrometer, magnet compensators, IT quadrupoles and correctors, separation/recombination dipoles, collimators and injection beam stoppers, the tunnel, and the experimental cavern with LHCb detector. The beam line has been modeled on both sides of Point 8 because of the left/right asymmetry of IR8. The machine model can be built automatically from the LHC optics files, once the description of the geometry, materials and magnetic field is available for each component [5].

Collision debris particles, produced in inelastic and diffractive collisions at the IP, have been simulated using the FLUKA built-in interface to DPMJET III [6]. Beam divergence and vertex position distributions have been implemented. For the final normalisation, we assumed 85 mb proton-proton cross-section [7].

The presence of the LHCb spectrometer produces 135 μrad kick in the horizontal plane for circulating 7 TeV proton beam, and is compensated with three dipoles, one (MBXWH) placed symmetrically with respect to the IP and two weaker dipoles (MBXWS) placed next to the IT. These dipoles play a major role in spreading collision debris particles in the horizontal plane and thus in affecting the energy deposition pattern. The internal crossing angle must be superimposed to the external crossing one defined by the optics. Two different configurations for the external crossing angle have been simulated: external angle a) on the horizontal plane; and b) on the vertical plane. In both cases, an external half-crossing angle of 200 μrad , representing the most pessimistic case from the debris impact point of view, was considered. Since the optics configuration of the IT quadrupoles Q1-Q2A-Q2B-Q3 is DFFD¹ in the horizontal plane for the outgoing beam, it allows to directly compare energy deposition losses in scenario a) with the ones in IR1, where the crossing is vertical and its optics configuration is DFFD in the vertical plane². Scenario b) has been considered since it is presently used in physics runs and is one of the requirements made for the LHCb upgrade [1].

¹D stands for defocusing, while F for focusing.

²IT beam screen orientation in IR8 is vertical, *i.e.* smallest aperture in the vertical plane, while in IR1 is horizontal, thus allowing a complete analogy between the two cases.

HEAT DEPOSITION

The energy deposition in the coils is scored using a 3D cylindrical mesh with about 10 cm longitudinal bins, 2-degree azimuthal bins. Steady-state heat loads are estimated via the peak power density ϵ_{max} averaged over the radial dimension of the innermost coil layer (12 and 15 mm for Q1-Q3 and Q2, respectively), that is the most exposed to the radiation field. In the following, error bars indicate statistical uncertainties.

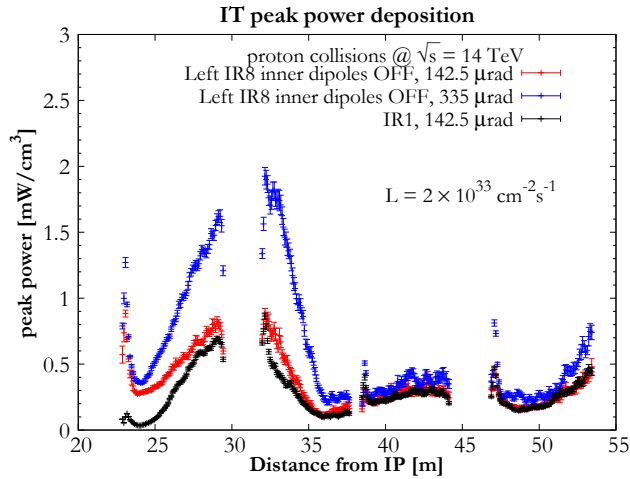


Figure 1: Longitudinal profile of ϵ_{max} along the IT quadrupoles: IR8 with 142.5 μrad half-crossing angle (red points); IR8 in the scenario (a) with 335 μrad half-crossing angle (blue points); IR1 with 142.5 μrad half-crossing angle (black points). The LHCb spectrometer and compensators have been set off. Results are normalized to $\mathcal{L}_{\text{max-LHCb}}$.

In the case of scenario (a), Fig. 1 shows the juxtaposition of the longitudinal profile of ϵ_{max} in IR8 with the one in IR1. For a sake of comparison, the LHCb spectrometer and compensators are switched off and all cases are normalized to $\mathcal{L}_{\text{max-LHCb}}$. Comparing IR8 (red profile) and IR1 (black), both with same crossing angle, it is evident that the effectiveness of the TAS is limited to the first half of Q1. Also looking at the total power deposited on the magnets, one can see that the TAS reduces by about one half the load on the Q1 with no significant effect on the rest of LSS magnets. On the other hand, the increase of the crossing angle (blue pattern) plays a much more dramatic role, enhancing the peak located at the end of Q1/beginning of Q2A, and in Q3.

In the more relevant scenario (b), with spectrometer and compensators switched on, the IR8 longitudinal profile of ϵ_{max} is shown in Fig. 2, for both right and left side of IP8. By comparing with scenario (a), it results that the role of the spectrometer and compensators is to increase the peak on the IP side of Q1 by about a factor 2, because low momentum particles (less than few hundred GeV) are sparsely scattered on the horizontal plane, thus hitting Q1 front face. The peak power in IT is about 2.2 mW/cm^3

and it is located on IP side of Q1 on the right side of IP8, because of the spectrometer larger aperture with respect to MBXWH dipole on the other side. As reference, in the scenario (a), the peak can be as high as 3.0 mW/cm^3 , because of the larger crossing angle on the horizontal plane. Considering now the separation dipoles, a peak power value approaching 1.5 mW/cm^3 has been estimated, located at the non IP side of D1, following the rise started in the Q3. Lastly, a peak by about 2.7 mW/cm^3 is located on the IP side of D2 left. The peak value on D2 right is lower, thanks to the presence of an additional shielding element, TCDD, that is a mask placed 3 m upstream of D1 right, to protect it by injection failure. In Refs. [1, 8], it is also stated that, due to the present beam screen orientation, an external crossing angle already at injection phase might have aperture limitation. Therefore, the rotation of the beam screen in IR8 is under discussion. Calculations show that this has only a minor effect on the peak power deposition pattern in the IT.

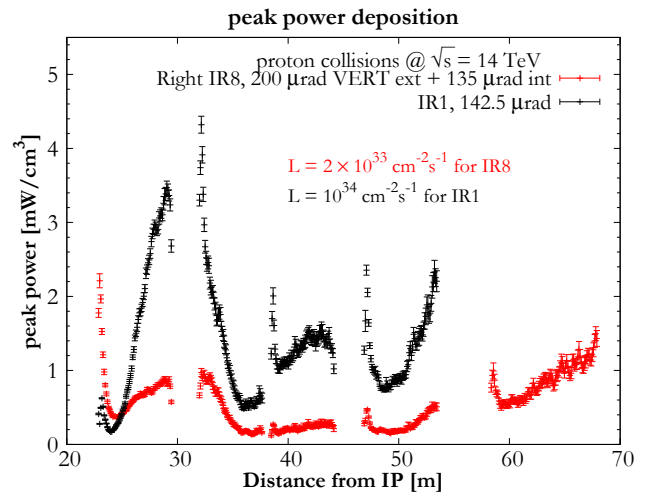


Figure 3: Longitudinal profile of ϵ_{max} along the IT quadrupoles and D1: IR1 with 142.5 μrad half-crossing angle at \mathcal{L}_0 (black points); IR8 in the scenario (b) at $\mathcal{L}_{\text{max-LHCb}}$ (red points). The D1 peak profile is shown only for IR8, because there is no equivalent in the high luminosity IRs, where D1 is a normal conducting magnet.

Figures 3 and 4 show the comparison of the IR8 case with the one of high luminosity IRs, all at their peak nominal luminosities (for the latter, $\mathcal{L}_0 = 10^{34} \text{ cm}^{-2} \text{ s}^{-1}$). We have chosen IR1 IT (its peak power is slightly higher with respect to IR5, due to the vertical crossing and DFFD optics configuration in the vertical plane), and IR5 D2 (debris particles not caught by IT are then lost in the Matching Section magnets, starting with D2). Power peak along IT and D1 are within the range of IR1, while the peak on the IP side of D2 is about five times higher than the case of the IR5. This peak is due to neutral particles flying directly from the IP and not intercepted before, because of the absence of the TAN.

Table 1 summarises total powers due to the collision debris on the most exposed magnets, and on the ensemble of

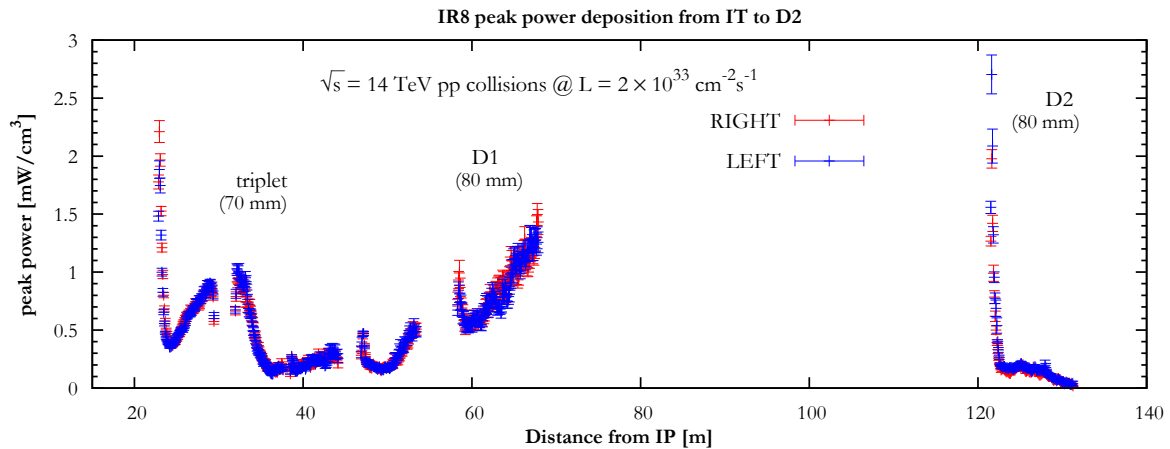


Figure 2: Longitudinal profile of ϵ_{max} from IT quadrupoles to D2 at $\mathcal{L}_{max-LHCb}$. Right (red) and left (blue) sides of IP8 are shown.

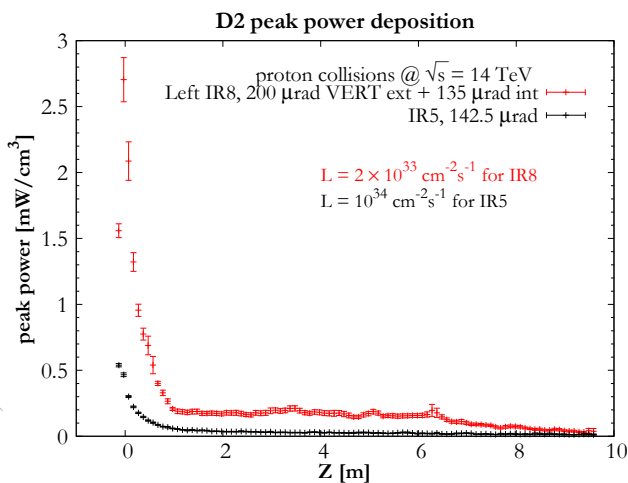


Figure 4: Longitudinal profile of ϵ_{max} along D2: IR5 with 142.5 μrad half-crossing angle at \mathcal{L}_0 (black points); IR8 in the scenario (b) at $\mathcal{L}_{max-LHCb}$ (red points).

the cryogenic magnets. The higher heat load on D2 in IR8 with respect to the ones in high luminosity IRs counsels to install a warm protection in front of D2.

Table 1: Total heat load

Magnet	IR8	IR1/5
	Power [W] at $\mathcal{L}_{max-LHCb}$	Power [W] at \mathcal{L}_0
Q1	30	43
D2	30	3
IT		150
IT & D1 (left/right)	50/60	

CONCLUSIONS

The LHCb luminosity upgrade to $2 \times 10^{33} \text{ cm}^{-2} \text{ s}^{-1}$ turns out to be compatible with no TAS installation, the role of which has been shown to be limited to the first IT quadrupole. The peak power in the IR8 magnets is

expected to be lower than in the IR1/5 triplets at \mathcal{L}_0 and within the quench design limit, that is considered to be 4.3 mW/cm³ for NbTi coils (including a safety factor of 3) [9].

A warm protection (TAN-like) is recommended to reduce the total load on the D2.

ACKNOWLEDGMENTS

We would like to thank R. De Maria, S. Fartoukh, S. Redaelli, L. Rossi for useful discussions, and the LHCb Collaboration for the FLUKA model of the detector.

REFERENCES

- [1] LHCb Collaboration, “Framework TDR for the LHCb Upgrade: Technical Design Report,” CERN-LHCC-2012-007, LHCb-TDR-12.
- [2] O. S. Brüning et al. (ed.), “LHC Design Report. 1. The LHC Main Ring,” CERN-2004-003-V-1, CERN-2004-003.
- [3] G. Battistoni et al., “The FLUKA code: Description and benchmarking,” AIP Conf. Proc. 896 (2007) 31.
A. Ferrari et al., “FLUKA: A multi-particle transport code (Program version 2005),” CERN-2005-010.
- [4] V. Vlachoudis, “FLAIR: A Powerful But User Friendly Graphical Interface For FLUKA,” Proc. Int. Conf. on Mathematics, Computational Methods & Reactor Physics (M&C 2009), Saratoga Springs, New York, 2009.
- [5] A. Mereghetti et al., “The FLUKA LineBuilder and Element DataBase: Tools for Building Complex Models of Accelerator Beam Lines”, IPAC2012, WEPPD071, p. 2687.
- [6] S. Roesler et al., “The Monte Carlo event generator DPMJET-III,” hep-ph/0012252.
- [7] J. Beringer et al., “Review of Particle Physics”, Phys. Rev. D 86, 010001 (2012).
- [8] B. J. Holzer et al., “Vertical Crossing Angle in IR8,” CERN-ATS-Note-2013-024.
- [9] N. V. Mokhov et al., “Protecting LHC IP1/IP5 Components Against Radiation Resulting from Colliding Beam Interactions,” Phys. Rev. STAB 9 (2006) 101001.